Biomechanical properties of the pelvic floor muscles of continent and incontinent women using an inverse finite element analysis

Article *in* Computer Methods in Biomechanics and Biomedical Engineering · March 2017

DOI: 10.1080/10255842.2017.1304542

CITATIONS
5

READS
104

5 authors, including:

Elisabete Silva
INEGI, Faculty of Engineering, University of Porto
37 PUBLICATIONS **46** CITATIONS
SEE PROFILE

Sofia Brandao
Hospital de São João
51 PUBLICATIONS **265** CITATIONS
SEE PROFILE

M. P. L. Parente
University of Porto
228 PUBLICATIONS **812** CITATIONS
SEE PROFILE

Teresa Mascarenhas
University of Porto
156 PUBLICATIONS **1,453** CITATIONS
SEE PROFILE

Taylor & Francis
Taylor & Francis Group

Computer Methods in Biomechanics and Biomedical Engineering

ISSN: 1025-5842 (Print) 1476-8259 (Online) Journal homepage: http://www.tandfonline.com/loi/gcmb20

Biomechanical properties of the pelvic floor muscles of continent and incontinent women using an inverse finite element analysis

M. E. T. Silva, S. Brandão, M. P. L. Parente, T. Mascarenhas & R. M. Natal Jorge

To cite this article: M. E. T. Silva, S. Brandão, M. P. L. Parente, T. Mascarenhas & R. M. Natal Jorge (2017): Biomechanical properties of the pelvic floor muscles of continent and incontinent women using an inverse finite element analysis, Computer Methods in Biomechanics and Biomedical Engineering

To link to this article: http://dx.doi.org/10.1080/10255842.2017.1304542

Published online: 17 Mar 2017.

COMPUTER METHODS IN BIOMECHANICS AND BIOMEDICAL ENGINEERING, 2017
http://dx.doi.org/10.1080/10255842.2017.1304542

Taylor & Francis
Taylor & Francis Group

Biomechanical properties of the pelvic floor muscles of continent and incontinent women using an inverse finite element analysis

M. E. T. Silva[a], S. Brandão[a,b], M. P. L. Parente[a], T. Mascarenhas[c] and R. M. Natal Jorge[a]

[a]LAETA, INEGI, Faculty of Engineering, University of Porto, Porto, Portugal; [b]Faculty of Medicine, Department of Radiology, Centro Hospitalar de São João-EPE, University of Porto, Porto, Portugal; [c]Faculty of Medicine, Department of Gynecology and Obstetrics, Centro Hospitalar de São João-EPE, University of Porto, Porto, Portugal

ABSTRACT

Pelvic disorders can be associated with changes in the biomechanical properties in the muscle, ligaments and/or connective tissue form fascia and ligaments. In this sense, the study of their mechanical behavior is important to understand the structure and function of these biological soft tissues. The aim of this study was to establish the biomechanical properties of the pelvic floor muscles of continent and incontinent women, using an inverse finite element analysis (FEA). The numerical models, including the pubovisceral muscle and pelvic bones were built from magnetic resonance (MR) images acquired at rest. The numerical simulation of Valsalva maneuver was based on the finite element method and the material constants were determined for different constitutive models (Neo-Hookean, Mooney-Rivlin and Yeoh) using an iterative process. The material constants (MPa) for Neo-Hookean (c_1) were 0.039 ± 0.022 and 0.024 ± 0.004 for continent *vs.* incontinent women. For Mooney-Rivlin (c_1) the values obtained were 0.026 ± 0.010 *vs.* 0.016 ± 0.003, and for Yeoh (c_1) the values obtained were 0.031 ± 0.023 *vs.* 0.016 ± 0.002, ($p < 0.05$). Muscle displacements obtained in the numerical simulations of Valsalva maneuver were compared with the muscle displacements obtained through additional dynamic MRI. Incontinent women presented a higher antero-posterior displacement than the continent women. The results were also similar between MRI and numerical simulations (40.27% *vs.* 42.17% for Neo-Hookean, 39.87% for Mooney-Rivlin and 41.61% for Yeoh). Using an inverse FEA coupled with MR images allowed to obtain the *in vivo* biomechanical properties of the pelvic floor muscles, leading to a relationship between them for the continent and incontinent women in a non-invasive manner.

ARTICLE HISTORY
Received 27 April 2016
Accepted 6 March 2017

KEYWORDS
Pelvic floor muscles; stress urinary incontinence; material constants; inverse finite element analysis

Introduction

The female pelvic floor is a support structure that includes fascia, ligaments and muscles (PFM) of the urogenital region. It extends from the *symphysis pubis* to the coccyx, and comprises the *levator hiatus* for the passage of the urethra, vagina and rectum. The group of *levator ani* muscle (the puborectal, pubococcygeal – that together form the pubovisceral – and iliococcygeal muscles; Schwertner-Tiepelmann et al. 2012) is one of the most important structures that support the pelvic organs (Barber et al. 2002). These muscles help maintaining the anorectal and urethral closure by resisting the downward forces imposed to the organs and the pelvic floor whenever the intra-abdominal pressure (IAP) is increased (Bø & Sherburn 2005; Schwertner-Tiepelmann et al. 2012).

The *levator ani* muscle differs from most other skeletal muscles in that it maintains a constant tone, except during voiding, defecation and Valsalva maneuver (Schwertner-Tiepelmann et al. 2012). Additionally, it has the ability to perform quick contractions in response to the sudden increase of the IAP, e.g. during cough, sneeze or physical activity, thereby maintaining continence and the pelvic organs in their anatomical positions (Schwertner-Tiepelmann et al. 2012).

The mechanical characteristics of the female pelvic floor are relevant to explain pelvic disorders (Barber et al. 2002). The decreased elasticity of the tissues often causes inability to maintain the normal positions of the pelvic organs. Pelvic floor disorders (PFD; Schwertner-Tiepelmann et al. 2012) may result from inadequate mechanical properties of the supportive structures such as the impairment of the muscles or ligaments, or changes in their stiffness, as well as those in the pelvic fascia, associated with changes in hormonal levels during pregnancy,

CONTACT M. E. T. Silva silva.elisabete3@gmail.com

vaginal delivery or menopause (Barber et al. 2002; Rahn et al. 2008; Abramowitch et al. 2009).

Urinary incontinence (UI) is the most common pelvic disorder among aging females, greatly affecting their quality of life. The most common type of UI in women is stress UI (SUI), defined as the complaint of involuntary leakage of urine (Bø 2004; Bø & Sherburn 2005) on effort or exertion, or on sneezing or coughing (Abrams et al. 2002; Thyer et al. 2008).

Previous works have shown that the decreased total collagen and elastin can be associated with the abnormalities in the pelvic ligaments (Chen & Yeh 2011) and fascia (Klutke et al. 2008), leading to loss of support and SUI and pelvic organ prolapse (POP) symptoms (Tinelli et al. 2010; Chen & Yeh 2011). This has also been studied through biomechanical modelling; the effect of structural degradation of the support structures such as the ligaments and fascia can be another ingredient to develop SUI and cystocele (Yip et al. 2014; Brandão, Parente, Rocha, et al. 2015). Furthermore, despite the proved association between SUI and direct damage to the pelvic floor muscles (often during vaginal delivery (DeLancey et al. 2007)), SUI is also associated with weakness of the *levator ani* complex, and poor function or decreased strength of the urethral sphincter, not always in the presence of PFM injury (McGuire 2004).

Magnetic resonance imaging (MRI) shows anatomic information on the *status* of the pelvic floor due to the high soft-tissue contrast, and the availability of acquiring functional (dynamic) images (Tunn et al. 1998; Majida et al. 2010). By performing these additional sagittal dynamic images during during Valsalva maneuver or straining one can evaluate the action of the PFM counteracting the increase in IAP (Peng et al. 2007; Yang et al. 2009). Additionally, to explore the stiffness of the PFM, imaging techniques based on ultrasound and MRI were used to compare continent and stress urinary incontinent women (Tunn et al. 1998; Dietz 2004; Dietz et al. 2008; Siegel et al. 2015).

The pelvic soft tissues are the major focus of several research groups (Janda 2006; Noakes et al. 2008; Parente, Natal Jorge, et al. 2009) have been studied, but since *in vivo* experimental studies are very difficult to undertake in this field, *ex vivo* studies or animal models allowed to determine the biomechanical properties (Rahn et al. 2008; Abramowitch et al. 2009). Furthermore, biomechanical models have been applied to better understand the role and the mechanical behavior of the pelvic structures in the development of UI and prolapse (Da Silva-Filho et al. 2010; Brandão et al. 2015), by using the material properties retrieved from experimental studies with both normal and pathological specimens (Rubod et al. 2012; Martins et al. 2013; Rivaux et al. 2013). More recently, computational model based on MR images of a young and asymptomatic and an inverse Finite Element Analysis (FEA) were used to determine *in vivo* biomechanical properties of the PFM for a non-pathologic case (Silva et al. 2016). In the same line, the aim of this work was to use identical methodology for two distinct groups (continent and incontinent women), by which the material constants for different constitutive models (Neo-Hookean, Mooney-Rivlin and Yeoh) for the passive behavior of the PFM were obtained. After the determination of the material constants, the displacement of the PFM at Valsalva maneuver was compared between the deformed numerical model and the dynamic MR images.

Methods

A set of women was asked to complete the International Consultation of Incontinence Questionnaire-Short Form (ICIQ-SF) – which is validated for the Portuguese language (Tamanini et al. 2004) – to evaluate the presence and symptoms of UI. In addition, demographic characteristics such as age, body mass index (BMI) and parity were obtained. For this work, the exclusion criteria included pregnancy and previous pelvic surgery. A convenient sample of 8 women who gave informed consent was recruited. Four incontinent women (with SUI) and other four continent women (control group) were recruited at a regular urogynecology consultation.

MR images acquisition and analysis

All women undertook a pelvic MR exam with multiplanar T2w images acquired in the supine position at rest using a 3T scanner (Magnetom® Tim Trio, Siemens Medical Solutions, Erlangen, Germany), along with cine images acquired at Valsalva maneuver.

Before the dynamic acquisitions acquired in the mid-sagittal plane, women were instructed on how to perform the Valsalva maneuver properly by a physiotherapist with 4 years knowledge in pelvic floor rehabilitation, as described elsewhere. The MR datasets used in this work were the same as previous works.

Figure 1 shows sagittal images at rest and at maximal Valsalva maneuver from two women, a continent 28-year-old ((a) and (b)), and an incontinent 30-year old ((c) and (d)).

To evaluate muscle displacement, horizontal and vertical axes (orange lines) were placed in the inferior and posterior border of the *symphysis pubis* (Peng et al. 2007; Brandão, Parente, Rocha, et al. 2015). The antero-posterior diameter of the *levator hiatus* – measured from the postero-inferior border of the *symphysis pubis* to the puborectal muscle (the main constrictor of the pelvic floor muscles; straight blue line) – and its vertical position

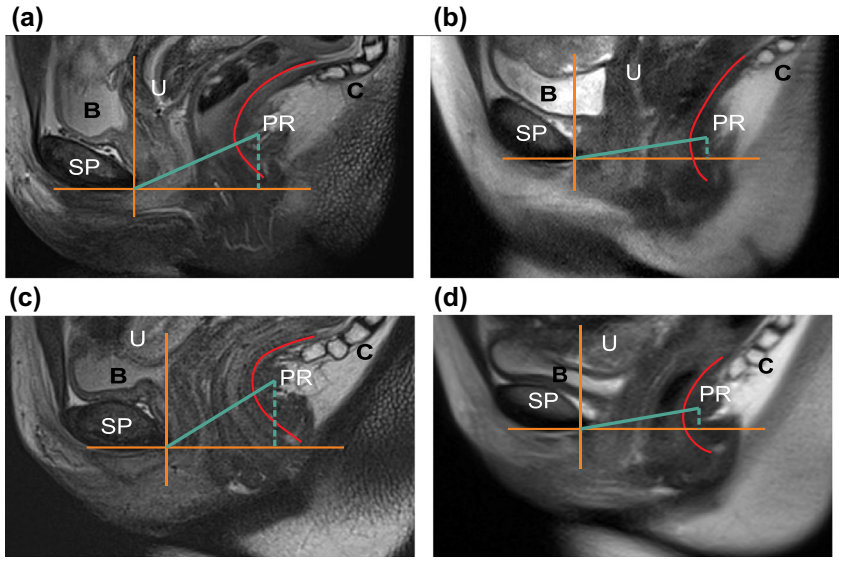

Figure 1. MR images in the mid-sagittal plane of a continent (a and b) and incontinent woman (c and d). Images acquired at rest position (a and c), and during maximal Valsalva maneuver (b and d).
Notes: The antero-posterior *levator hiatus* displacement (straight blue line) and the supero-inferior displacement of the puborectal muscle (dashed blue line). B – bladder; C – coccyx; PR – puborectal muscle; SP – *symphysis pubis*; U – uterine cervix.

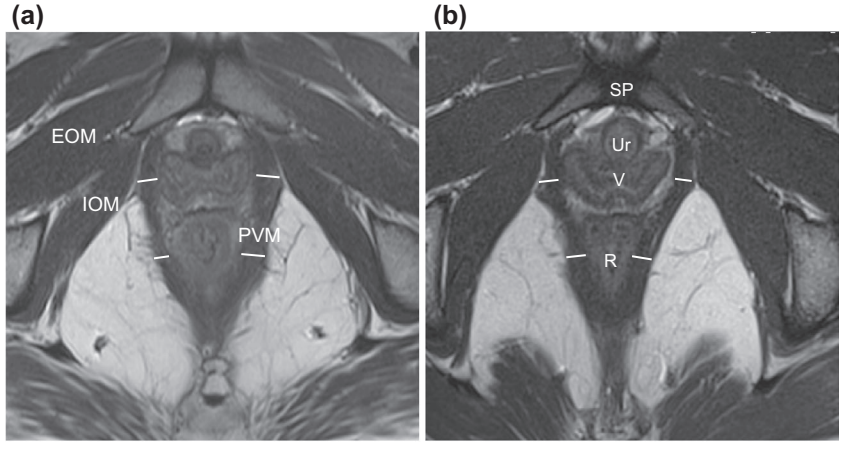

Figure 2. Magnetic resonance images in the axial plane of a continent (a) and incontinent woman (b).
Notes: The measurements of muscle thickness were made at the level of the midvagina and the anal canal. EOM – external obturator muscle; IOM – internal obturator muscle; PVM – pubovisceral muscle; R – rectum; SP – *symphysis pubis*; Ur – urethra V – vagina.

(dashed blue line) were assessed. The displacement in the antero-posterior axis was considered as the difference between the length of the straight blue line between the images acquired at rest and Valsalva.

During Valsalva maneuver, the descent of the organs along the horizontal axis is verified, along with the widening of the *levator hiatus* in some degree, and opening of the anorectal angle, which is accompanied by some degree of verticalization of the *levator plate* (Tumbarello et al. 2010; Brandão et al. 2015). Previous works on clinical dynamic MR imaging (Raizada & Mittal 2008) and numerical simulation (Noakes et al. 2008) described these features. The red lines illustrated in Figure 1 were used to compare the position of the anorectal angle and *levator plate* at rest *vs.* Valsalva maneuver.

The T2w axial images were used to measure the pubovisceral muscle thickness at the level of the midvagina and anal canal for the continent and incontinent women (Figure 2 (a) and (b)). The plane of minimal hiatal dimensions was used to measure the thickness, such as described by Majida et al. (2010) and Da Roza et al. (2015).

Numerical simulation

The biomechanical models of the pubovisceral muscle and the surrounding bone structures were built from

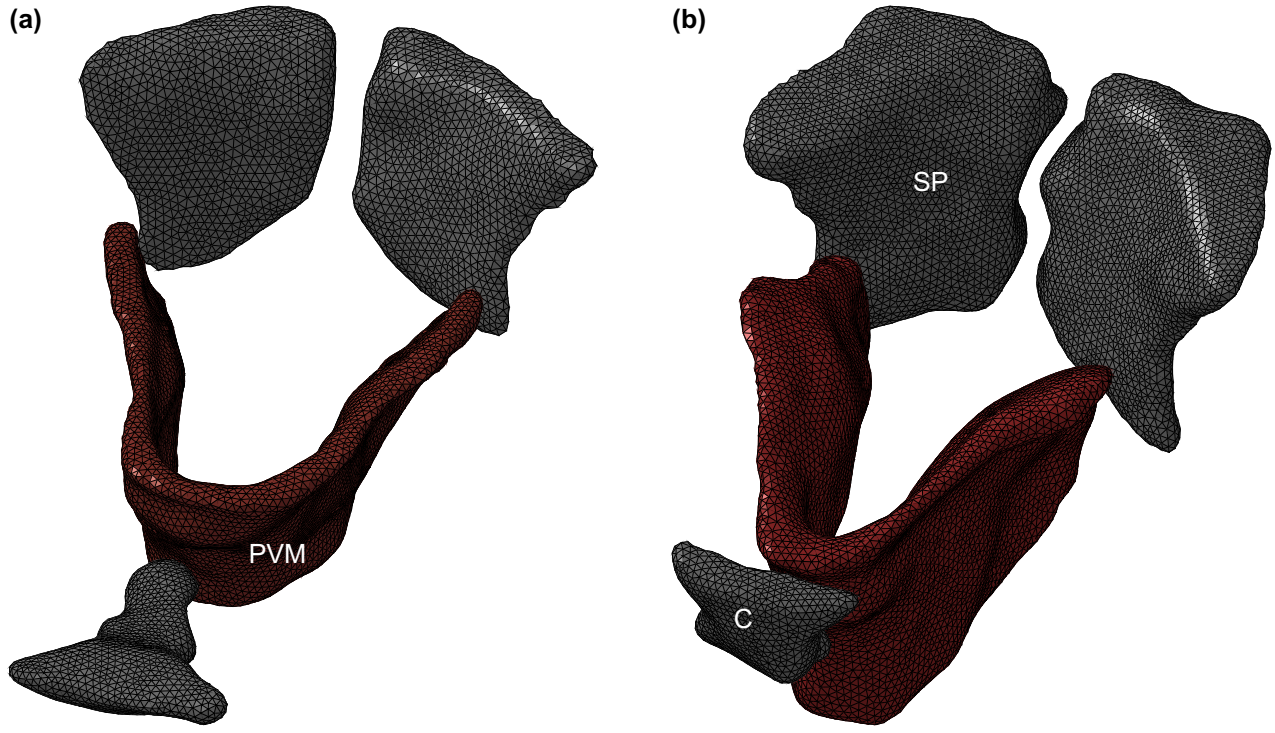

Figure 3. Finite element mesh built from the MR axial images of a continent (a) and an incontinent woman (b).
Note: C – coccyx; PVM – pubovisceral muscle; SP – *symphysis pubis*.

the axial images. The 3D solid models of these structures were obtained by applying a semi-automatic procedure using the Mimics® software v.16 (Software and Services for Biomedical Engineering, Materialise HQ, Belgium), as in previous work (Silva et al. 2016). After this procedure, the geometrical model of the muscle and the finite element mesh (with hybrid tetrahedral elements – C3D4H) were created using the Abaqus software v.6.12 (Dassault Systmes Simulia Corp., Providence, RI, USA; see Figure 3). The number of elements and volume in the meshes varied among the subjects due to the individual differences in the muscle geometry.

To simulate Valsalva maneuver, the boundary conditions to the pubovisceral muscle were imposed to incorporate the existence of the surrounding structures – *symphysis pubis*, internal obturator fascia and coccyx, visualized in the MR images. The nodes corresponding to the insertion of the pubovisceral muscle in the different structures were considered fixed (Parente et al. 2008; Parente, Jorge, et al. 2009; Rubod et al. 2012). A pressure of the 4 kPa was applied to the inner surface of the muscle, following the methodology described by Noakes et al. (2008).

The inverse finite element analysis

In this work, an inverse FEA implemented by Silva et al. (Silva et al. 2016) was used to obtain the material constants for different constitutive models (Neo-Hookean, Mooney-Rivlin and Yeoh). The inverse FEA uses the optimization algorithm to search for the most suited set of material constants of the different constitutive models, in order to minimize its objective function (Powell 1977; Gao et al. 2013), by allowing the minimum distance between the two reference curves drawn on Figure 1 for each subject (Figure 4). One curve represents the position of the puborectal muscle in the numerical model for each iteration and related deformation, and the other curve represents its position in the dynamic mid-sagittal image acquired at Valsalva maneuver. The Powell optimization algorithm was used because it does not calculate the gradient and it is one of the most efficient, reliable and also one of the most widely known of the zero-order methods (Powell 1977).

The inverse FEA was used to obtain the suited material constants for the different constitutive models by using the Python scripting language to couple with the MATLAB MathWorks v. R2013b (Mathematical Computing Software, Natick, Massachusetts, USA) and the Abaqus software. A Python script was used to update the displacements of the nodes along a portion of the curve representing the position of the puborectal muscle on the numerical model for each simulation (see Figure 4).

The error measure represents the sum of all the distances between the two curves and the stopping criteria was set to <10 mm. Equation (1) (Silva et al. 2016).

$$\text{Error} = \sum_{i=1}^{np} \left\| d_{\text{MRI}_i} - d_{\text{FEA}_i} \right\| \quad (1)$$

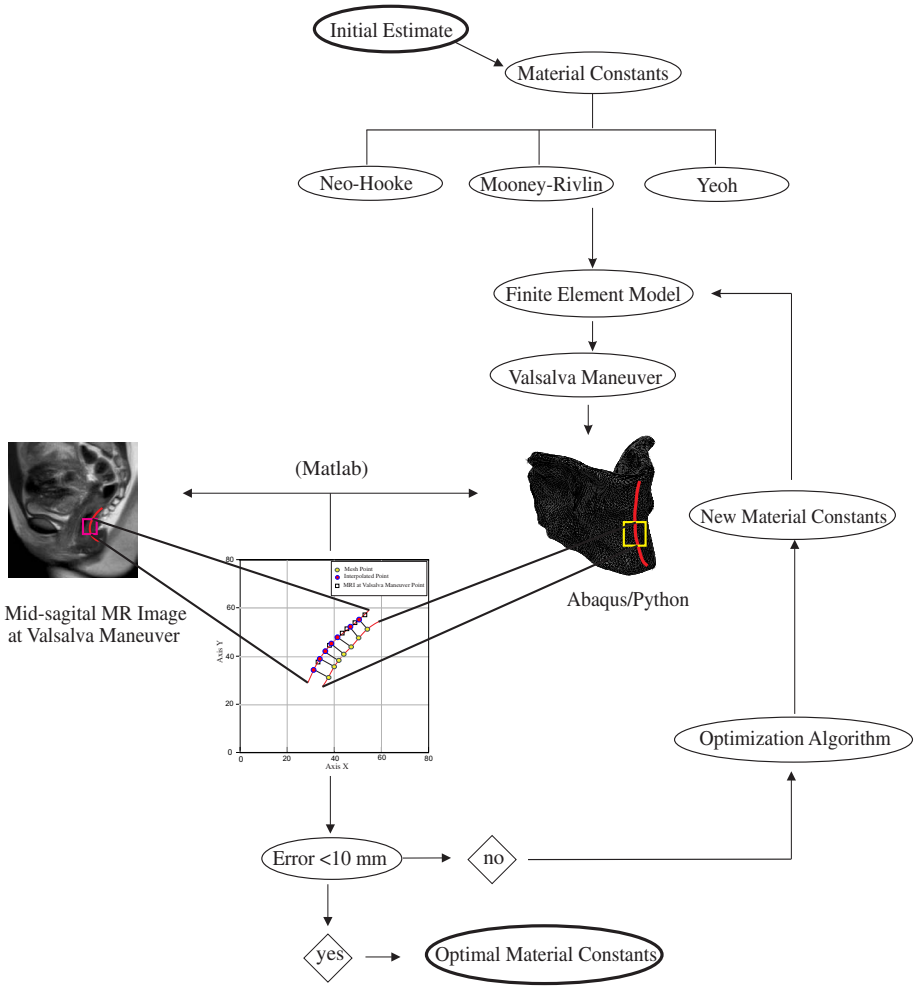

Figure 4. Flow chart of the inverse FEA applied to obtain the material constants of the Neo-Hooke, Mooney-Rivlin and Yeoh constitutive models.

By applying an iterative process, the most suited material constants were found, corresponding to the ones in the iteration with a minimum error.

In order to simulate the mechanical behavior of the skeletal pubovisceral muscle – which was considered fully incompressible – the following distinct constitutive models were used (Neo-Hookean, Mooney-Rivlin and Yeoh) for two main reasons: firstly because they are simple models (with few constants to optimize) that employ a nonlinear relationship between stress and strain to describe incompressible hyperelastic materials, and also because they have proved to correctly describe the biomechanical behavior of the PFM during simulation of Valsalva maneuver and defecation (Lee et al. 2005; Janda 2006; Noakes et al. 2008), and vaginal delivery (Li et al. 2008).

The Neo-Hookean (Equation 2), Mooney-Rivlin (Equation 3) and Yeoh (Equation 4), constitutive models are characterized by:

$$W = c_1(I_1 - 3) \tag{2}$$

$$W = c_1(I_1 - 3) + c_2(I_2 - 3) \tag{3}$$

$$W = c_1(I_1 - 3) + c_2(I_2 - 3)^2 + c_3(I_3 - 3)^3 \tag{4}$$

where W is the strain energy function and c_1, c_2 and c_3 are the material constants to be determined and have dimensions of stress, I_1, I_2 and I_3 are the principal strain invariants (Equation 5) of the right Cauchy-Green tensor (Noakes et al. 2008). For the case uniaxial stretching, the principal strain invariants are represented as follows:

$$\begin{aligned} I_1 &= \lambda^2 + \tfrac{2}{\lambda} \\ I_2 &= 2\lambda + \tfrac{1}{\lambda^2} \\ I_3 &= 1 \end{aligned} \tag{5}$$

where λ is the maximum principal stretch.

In the case of uniaxial stretching, the Cauchy stress σ, a function of the invariants (Equation 6), can be described by the following equation (Martins et al. 2006):

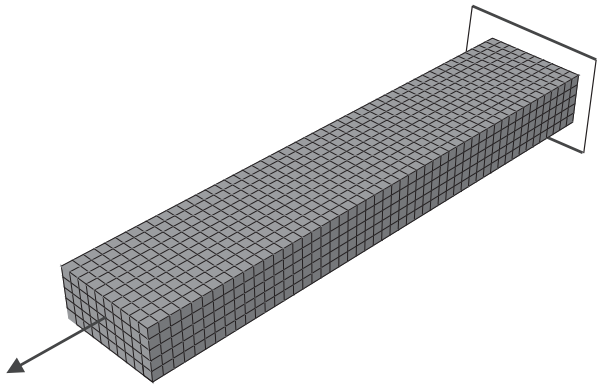

Figure 5. Finite element model used to obtain numerical stress-strain response.

$$\sigma = 2\left(\lambda^2 - \frac{1}{\lambda}\right)\left(\frac{\partial W}{\partial I_1} + \frac{1}{\lambda}\frac{\partial W}{\partial I_2}\right) \tag{6}$$

The particular expression of the Cauchy stresses is obtained for each material constitutive model depending on the invariants. The Neo-Hookean material model depends on the invariant I_1 (Equation 2), so the Cauchy stress obtained using Equation (6) is,

$$\sigma_{\text{Hookean}} = 2\left(\lambda^2 - \frac{1}{\lambda}\right)c_1 \tag{7}$$

The Mooney-Rivlin material model also depends on the invariants I_1 and I_2 (Equation 3), and also enables the use of the Equation (6) to obtain the Cauchy stress represented in Equation (8),

$$\sigma_{\text{Mooney}} = 2\left(\lambda^2 - \frac{1}{\lambda}\right)\left(c_1 + c_2\frac{1}{\lambda}\right) \tag{8}$$

The Cauchy stress for Yeoh material model is,

$$\sigma_{\text{Yeoh}} = 2\left(\lambda^2 - \frac{1}{\lambda}\right)\left(c_1 + 2c_2\left(I_1 - 3\right) + 3c_3\left(I_1 - 3\right)^2\right) \tag{9}$$

In order to check the usefulness of the established parameters, a numerical simulation representing a uniaxial tensile test was performed. Figure 5 shows the finite element model to obtain the numerical stress-strain response. This numerical model was created with 3366 nodes and 2500 elements. The FEM was generated by using hybrid linear tetrahedral elements (Abaqus C3D8H). The element size set was approximately constant throughout the geometry, resulting in a mesh with a characteristic element length of 1.0 mm.

The continuous variables were described by means of the mean value and standard deviation (SD). The demographic features, the morphological characteristics of the muscle and its displacement for Valsalva maneuver, and also the material constants of the three different constitutive models were compared between two groups by using the Mann-Whitney *U* test. A p value of <0.05 was considered statistically significant. All analyses were computed using IBM SPSS Statistics 23.0 software.

Table 1. Demographic characteristics and muscle morphological features for the two groups.

Variable		CG ($n = 4$)	IG ($n = 4$)	p value
Age		30.50 ± 10.44	30.75 ± 21.67	0.486
BMI		24.62 ± 4.61	22.23 ± 4.13	0.343
Parity		0.50 ± 1.00	0.50 ± 1.00	1.000
Thickness (mm)	MidVa (left)	8.12 ± 2.00	5.43 ± 1.50	0.200
	MidVa (right)	7.29 ± 2.28	5.95 ± 1.63	0.343
	AC (left)	5.20 ± 1.27	4.14 ± 1.01	0.486
	AC (right)	5.68 ± 1.78	4.28 ± 0.26	0.343

Note: AC: anal canal; BMI: body mass index; CG: continent group; IG: incontinent group; MidVa: midvagina; mm: millimeters.

Results

Demographic and morphological characteristics of the continent and incontinent women are presented in Table 1. When comparing the two groups, no significant difference in age, BMI, parity and muscle thickness were found.

Table 2 presents the mean values of the material constants for three different constitutive models obtained by inverse FEA, which show significant differences.

Figure 6 shows the stress-stretch response for the study of the nonlinear mechanical behavior of the uniaxial tension test with the means values of the material constants obtained for the continent (a) and incontinent (b) women. The results correspond to the comparison between uniaxial tension tests obtained analytically from the Equations (7), (8) and (9) and those obtained numerically through the simulations.

Figure 7 presents the mechanical response of the uniaxial stress-stretch response from continent and incontinent women to compare the effect of material constants (Table 2) obtained in this work with other material constants existing in literature. The material constants for the Yeoh constitutive model of the table in Figure 7 were estimated in the Abaqus software through experimental curves (softer and stiffer) extracted from cadaveric muscle (Janda 2006). All the experimental/numerical curves were compared with the analytical curves from Equations (7)–(9). The continent group showed higher values for the stress (MPa). The curve of the Yeoh constitutive model for the continent women follows the non-linear behavior of the stiffer experimental curve, and the curves for the incontinent women follow the behavior of the softer experimental and Neo-Hookean curve of the literature. The maximum stress values are higher for the continent women and for the three constitutive models.

Table 2. Material constants of the pubovisceral muscle in women with and without UI, and variation between the groups.

Variable		CG ($n = 4$)	IG ($n = 4$)	p value	Variation (%)
Neo-Hookean	c_1(MPa)	0.039 ± 0.022	0.024 ± 0.004	0.029*	38.46%
Mooney-Rivlin	c_1(MPa)	0.026 ± 0.010	0.016 ± 0.003	0.029*	38.46%
	c_2(MPa)	0.014 ± 0.014	0.005 ± 0.001	0.029*	64.29%
Yeoh	c_1(MPa)	0.031 ± 0.023	0.016 ± 0.002	0.029*	48.39%
	c_2(MPa)	0.025 ± 0.028	0.004 ± 0.001	0.029*	84.00%
	c_3(MPa)	0.023 ± 0.038	0.001 ± 0.001	0.029*	95.65%

Notes: CG: continent group; IG: incontinent group.
*statistically significant.

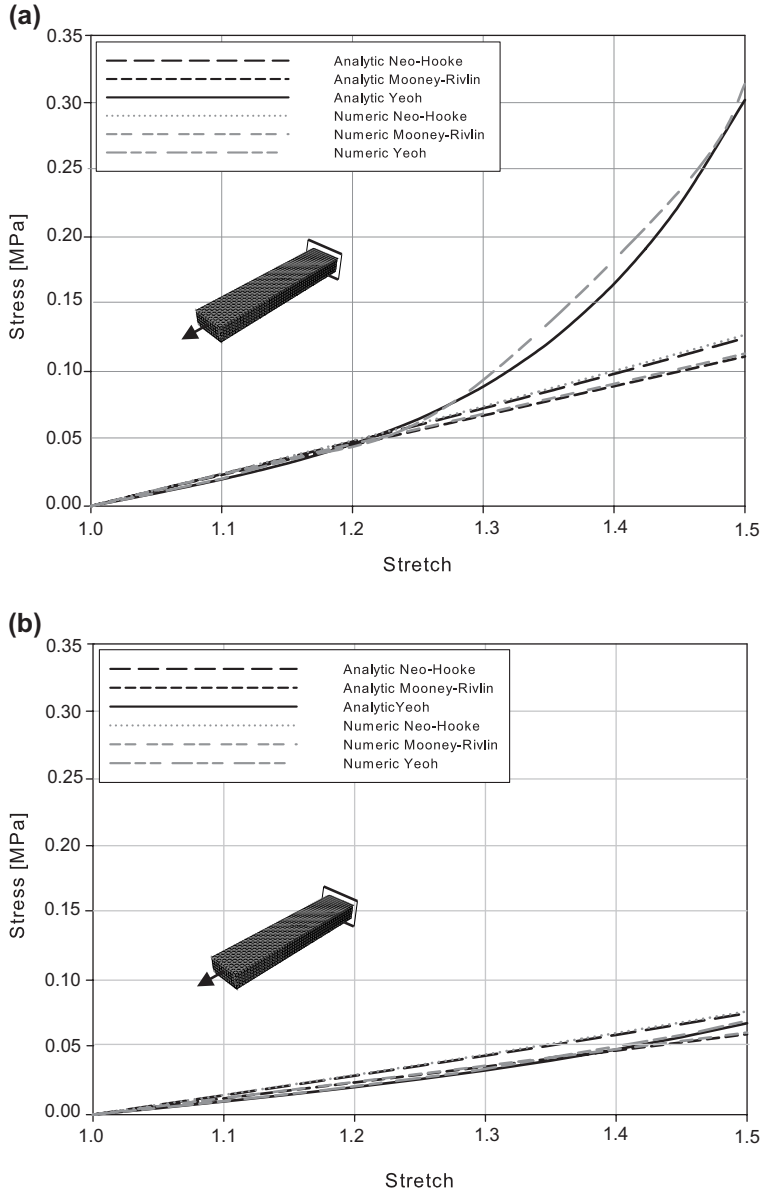

Figure 6. Stress-stretch response for passive behavior of the pubovisceral muscle for the different constitutive models. (a) for the continent and (b) for the incontinent group. The response obtained analytically and numerically was compared.

Table 3 presents the displacement of the pubovisceral muscle in the numerical simulation *vs.* MRI, as represented by the posterior and inferior movement. The displacements obtained in the numerical simulation were similar with the one obtained in the dynamic MRI for the three constitutive models (p-values > 0.05). When comparing the two groups, the difference for the antero-posterior displacement for continent and incontinent women was approximately 42.17% for the Neo-Hookean, 39.87% for the Mooney-Rivlin and 41.61% for the Yeoh models, respectively,

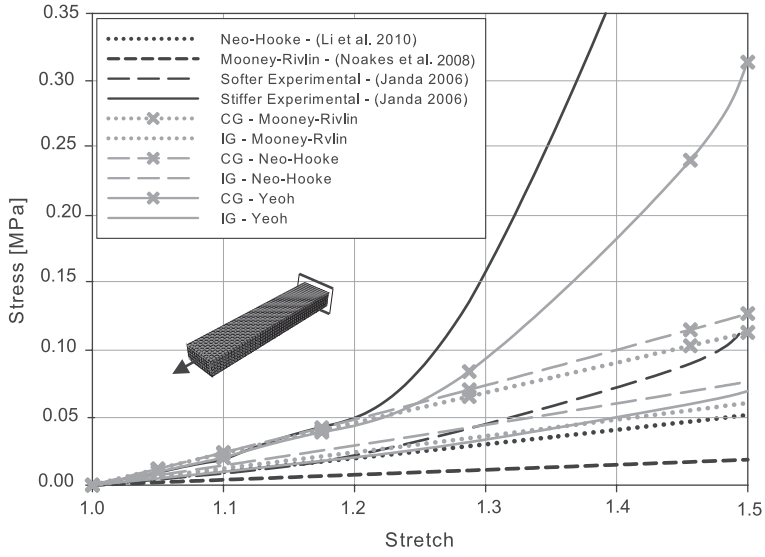

Model	c_1 *(MPa)*	c_2 *(MPa)*	c_3 *(MPa)*	*Experimental/Numerical data*
Neo-Hooke	1.61E-02	……..	……..	(Li et al. 2010)
Mooney-Rivlin	4.50E-03	2.00E-03	……..	(Noakes et al. 2008)
Yeoh (softer curve)	1.31E-02	1.49E-02	2.79E-02	(Janda 2006)
Yeoh (stiffer curve)	2.87E-02	8.21E-02	9.36E-02	

Figure 7. Uniaxial stress–stretch response for passive behavior of the pubovisceral muscle for the different constitutive models and experimental/numerical data of the literature.

Table 3. Displacements of the dynamic MRI compared with the displacements of the numerical models for two groups of women.

Variable	MRI (mm)	Neo-Hookean (mm)	Mooney-Rivlin (mm)	Yeoh (mm)
CG-AP	4.495 ± 1.560	4.475 ± 1.534	4.755 ± 1.529	4.630 ± 1.366
IG-AP	7.525 ± 1.306	7.738 ± 1.984	7.908 ± 1.698	7.930 ± 1.651
p value	0.057	0.114	0.057	0.057
Variation (%)	40.27%	42.17%	39.87%	41.61%
CG-SI	6.235 ± 4.004	4.768 ± 3.503	5.113 ± 3.818	4.983 ± 3.387
IG-SI	5.845 ± 2.238	4.020 ± 2.355	4.235 ± 2.004	4.435 ± 1.742
p value	1.000	0.886	1.000	1.000
Variation (%)	6.34%	15.69%	17.17%	11.00%

Notes: CG-AP: continent group – antero-posterior; CG-SP: continent group – supero-inferior; IG-AP: incontinent group – antero-posterior; IG-SP: incontinent group – supero-inferior.

and the supero-inferior displacement was approximately 15.69% for the Neo-Hookean, 17.17% for the Mooney-Rivlin and 11.00% for the Yeoh models, respectively. The horizontal displacement measured in the MR images was 40.27% higher in incontinent women while the one along the vertical axis was 6.34% higher for the continent women.

Figure 8 shows the contour of the pubovisceral muscle to better illustrate the displacement for the three constitutive models, (a) Neo-Hookean, (b) Mooney-Rivlin and (c) Yeoh. Since the morphological analysis showed no significant differences between groups, a pubovisceral muscle of a continent woman was used to analyse the influence of using the three constitutive models. The figure shows the contour at rest position and Valsalva maneuver achieved through of the material constants obtained for continent group and incontinent group (Table 2). When comparing the three constitutive models, the displacement between Neo-Hookean and Mooney-Rivlin was similar, but it tends to be a little bit greater when using the material constants of the Yeoh constitutive model for incontinent group.

Discussion

UI may be considered as the consequence of the alteration of a biomechanical process (McGuire 2004). The nerves, muscles and connective tissues are responsible for

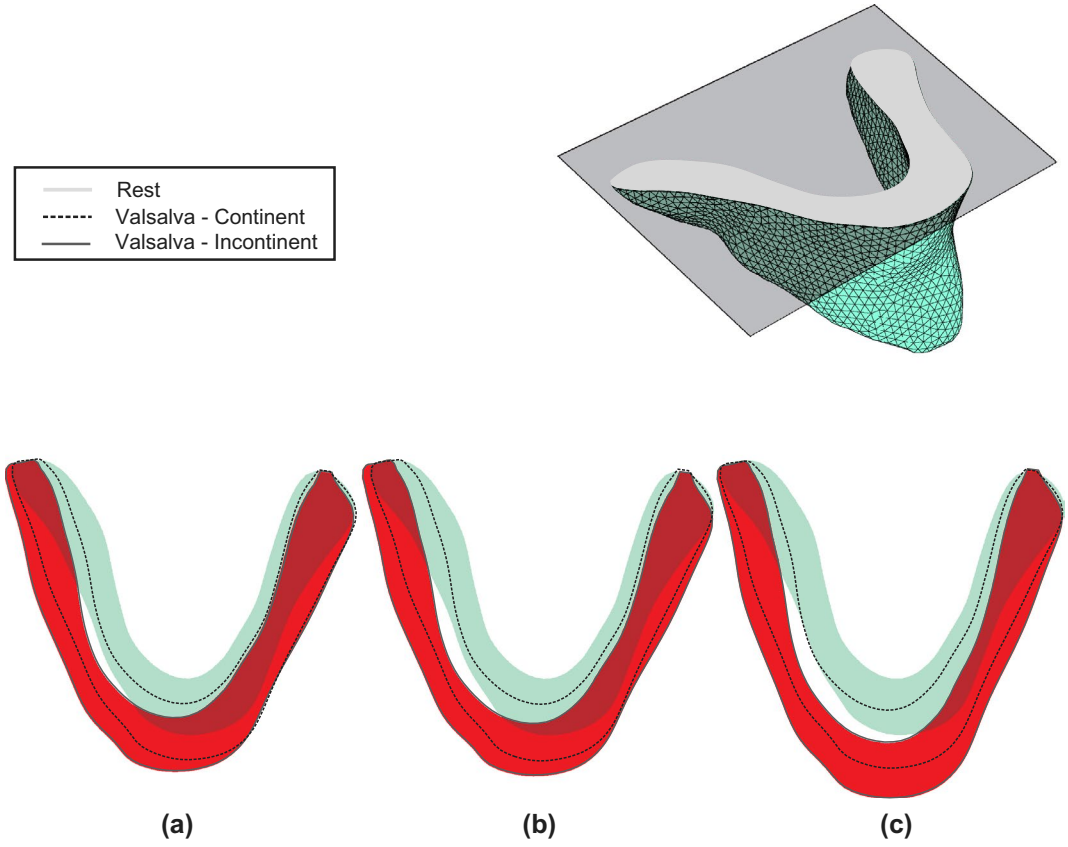

Figure 8. Pubovisceral muscle contour for a continent woman using Neo-Hooke (a), Mooney-Rivlin (b) and Yeoh (c) constitutive models.

maintaining continence, providing resistance to downward displacements during increase in IAP (Denise et al. 2000).Their biomechanical properties are proven to be relevant to explain the pelvic disorders (Derpapas 2015).

In the present work, an inverse FEA was used to obtain the most suited biomechanical properties of the pubovisceral muscle for continent and incontinent women, using an optimization algorithm coupled with the FEM in a completely non-invasive way.

There were no significant differences in the demographic characteristics or in the morphological measurements of muscle between continent and incontinent women. Therefore, the higher anterior-to-posterior displacement, corresponding to the opening of the *levator hiatus* in incontinent women can be associated with changes in the biomechanical properties of the pelvic floor muscles. Previous studies show that women with SUI present a significant reduction of type III collagen, which is not due to a decreased production of collagen but due to increased degradation of nascent collagen (Patel et al. 2007). Also, Rechberger et al. showed that weakening of the collagen framework of the pubovisceral fascia affects women of all ages (Rechberger et al. 1998).

The values of the material constants are significantly higher for the continent than for the incontinent women. The variation for continent *vs.* incontinent group was approximately 38.46% for the c_1 for the Neo-Hookean, 38.46 and 64.29% for c_1 and c_2 of the Mooney-Rivlin, and 48.39, 84.00 and 95.65% for c_1, c_2 and c_3 of the Yeoh. Assuming that the c_1 has greater influence in the mechanical behavior (Noor & Mahmud 2015), the variation of this material constant for the three constitutive models are in accordance with the variation of the antero-posterior displacement – 42.17% for the Neo-Hookean, 39.8% for the Mooney-Rivlin and 41.6% for the Yeoh, respectively. Incontinent women have an antero-posterior displacement higher than continents, as previously described (Peng et al. 2007). Comparing the muscle displacement through numerical simulation *vs.* dynamic MRI during Valsalva maneuver, the values of antero-posterior was similar in the two methods for the two groups. The lower variation in the supero-inferior displacement between the methods can be associated with assumptions and simplifications in the model, as for example, due to the fixed boundary conditions in the obturator fascia.

Despite the limitations mentioned above, the numerical results were concordant with the analytical results, as shown in Figure 6, and the uniaxial stress-stretch response presented in this work shows that the values of

the material constants for the different constitutive models can be compared with the experimental/numerical data existent in the literature.

To properly interpret our findings, it is important to consider the limitations and simplifications involved. Firstly, this sample is small, secondly, the numerical models did not include the connective tissues (fascia and ligaments) and pelvic organs, which would be more realistic.

Taking these limitations into account, the inverse FEA could be used as a means to evaluate the changes in PFM after conservative treatment via a longitudinal evaluation, by associating changes in thickness and strength measured through results of muscle contraction and strength from the Oxford Grading Scale in the vaginal palpation, the increase in muscle thickness and improved *levator hiatus* closure from dynamic MRI, and the changes in the material constants throughout the process. On the other hand, when there is not evidence of clinical improvement, surgical treatment with synthetic slings is always an option. In those cases, by knowing the stiffness of the native tissue, subject-specific adequacy of the mesh material properties could be an issue in the future.

In conclusion, the inverse FEA used in this study allowed establishing the material constants of the female PFM for continent and incontinent women, which substantiated more realistic results. With the most suited material properties the results of numerical simulation *vs*. muscle displacement in dynamic MRI were similar. Nevertheless, material properties for women of the incontinent group were lower, which means softer muscles, and that is clinically reasonable. Furthermore, it is corroborated by the fact that incontinent women showed higher hiatal opening at maximal Valsalva maneuver in both dynamic MRI and numerical simulation.

Conflict of Interest Statement

The authors declare that there is no financial, professional or other personal interest of any nature or kind in any product, service and/or company that could be constructed as influencing the position.

Funding

This work was supported by the Ministério da Ciência Tecnologia, e Ensino Superior, FCT, Portugal, [grant number SFRH/BD/89519/2012], [grant number IF/00159/2014], [project number UID/EMS/50022/2013]; Project NORTE-01-0145-FEDER-000022 – SciTech – Science and Technology for Competitive and Sustainable Industries, cofinanced by Programa Operacional Regional do Norte (NORTE2020), through Fundo Europeu de Desenvolvimento Regional (FEDER).

ORCID

M. P. L. Parente http://orcid.org/0000-0002-3326-6345
R. M. Natal Jorge http://orcid.org/0000-0002-7281-579X

References

Abramowitch SD, Feola A, Jallah Z, Moalli PA. 2009. Tissue mechanics, animal models, and pelvic organ prolapse: a review. Eur J Obstet Gynecol Reproductive Biol. 144:S146–S158.

Abrams P, Cardozo L, Fall M, Griffiths D, Rosier P, Ulmsten U, Van Kerrebroeck P, Victor A, Wein A. 2002. The standardisation of terminology in lower urinary tract function: report from the standardisation sub-committee of the International Continence Society. Neurourol Urodyn. 21:37–49.

Barber MD, Bremer RE, Thor KB, Dolber PC, Kuehl TJ, Coates KW. 2002. Innervation of the female levator ani muscles. Am J Obstet Gynecol. 187:64–71.

Bø K. 2004. Pelvic floor muscle training is effective in treatment of female stress urinary incontinence, but how does it work? Int Urogynecol J Pelvic Floor Dysfunction. 15:76–84.

Bø K, Sherburn M. 2005. Evaluation of female pelvic-floor muscle function and strength. Phys Ther. 85:269–282.

Brandão FS, Parente MP, Rocha PA, Saraiva MT, Ramos IM, Natal Jorge RM. 2015. Modeling the contraction of the pelvic floor muscles. Comput Methods Biomech Biomed Eng. 8:1–10.

Brandão S, Parente M, Mascarenhas T, da Silva ARG, Ramos I, Jorge RN. 2015. Biomechanical study on the bladder neck and urethral positions: simulation of impairment of the pelvic ligaments. J Biomech. 48:217–223.

Chen B, Yeh J. 2011. Alterations in connective tissue metabolism in stress incontinence and prolapse. J Urol. 186:1768–1772.

Da Roza T, Brandão S, Oliveira D, Mascarenhas T, Parente M, Duarte JA, Jorge RN. 2015. Football practice and urinary incontinence: relation between morphology, function and biomechanics. J Biomech. 48:1587–1592.

DeLancey JOL, Miller JM, Kearney R, Reddy P, Umek W, Guire KE, Margulies RU, Ashton-miller JA. 2007. Vaginal birth and *de novo* stress incontinence: relative contributions of urethral dysfunction and mobility. Obstet Gynecol. 110:354–362.

Da Silva-Filho AL, Martins PALS, Parente MP, Saleme CS, Roza T, Pinotti M, Mascarenhas T, Jorge RMN. 2010. Translation of biomechanics research to ur ogynecology. Archives of Gynecology and Obstetrics. 282:149–155.

Denise H, Janis MM, DeLancey JOL, James AA-M. 2000. Differential effects of cough, valsalva, and continence status on vesical neck movement. Obstet Gynecol. 95:535–540.

Derpapas A. 2015. The use of imaging in the diagnosis of lower urinary tract disorders and pelvic organ prolapse in women [Thesis]. Imperial College London Department of Surgery & Cancer.

Dietz HP. 2004. Ultrasound imaging of the pelvic floor. Part II: three-dimensional or volume imaging. Ultrasound Obstet Gynecol. 23:615–625.

Dietz HP, Shek C, De Leon J, Steensma AB. 2008. Ballooning of the levator hiatus. Ultrasound Obstet Gynecol. 31:676–680.

Gao W, Liu S, Huang L. 2013. A novel artificial bee colony algorithm with Powell's method. Appl Soft Comput. 13:3763–3775.

Janda S. 2006. Biomechanics of the pelvic floor musculature [PhD. Thesis]. Technische Universiteit Delft.

Klutke J, Ji Q, Campeau J, Starcher B, Carlos Felix J, Stanczyk F, Klutke C. 2008. Decreased endopelvic fascia elastin content in uterine prolapse. Acta Obstet Gynecol Scand. 87:111–115.

Lee S, Darzi A, Yang G. 2005. Subject specific finite element modelling of the levator ani. Med Image Comput Computer-Assisted Intervention. 3749:360–367.

Li X, Kruger JA, Chung JH, Nash MP, Nielsen PMF. 2008. Modelling childbirth: comparing athlete and non-athlete pelvic floor mechanics. Med Image Comput Comput – Assist Interv. 11:750–757.

Majida M, Brækken IH, Bø K, Šaltyte Benth J, Engh ME. 2010. Validation of three-dimensional perineal ultrasound and magnetic resonance imaging measurements of the pubovisceral muscle at rest. Ultrasound Obstet Gynecol. 35:715–722.

Martins P, Jorge RN, Ferreira A. 2006. A comparative study of several material models for prediction of hyperelastic properties: application to silicone-rubber and soft tissues. Strain. 42:135–147.

Martins P, Lopes Silva-Filho A, Rodrigues Maciel Da Fonseca AM, Santos A, Santos L, Mascarenhas T, Natal Jorge RM, Ferreira AJM. 2013. Biomechan ical properties of vaginal tissue in women with pelvic organ prolapse. Gynecologic and Obstetric Investigation. 75:85–92.

McGuire EJ. 2004. Pathophysiology of stress urinary incontinence. Rev Urol. 6:S11–S17.

Noakes KF, Pullan AJ, Bissett IP, Cheng LK. 2008. Subject specific finite elasticity simulations of the pelvic floor. J Biomech. 41:3060–3065.

Noor SNAM, Mahmud J. 2015. Skin Prestretch Evaluation Adapting Mooney-Rivlin Model. Journal of Medical and Bioengineering. 4:31–35.

Tamanini JT, Dambros M, D'Ancona CAL, Palma PC, Rodrigues Netto N. 2004. Validation of the 'International Consultation on Incontinence Questionnaire – Short Form' (ICIQ-SF) for Portuguese. Rev Saude Publica. 38:438–444.

Parente M, Natal Jorge R, Mascarenhas T, Fernandes A, Martins J. 2008. Deformation of the pelvic floor muscles during a vaginal delivery. Int Urogynecol J Pelvic Floor Dysfunction. 19:65–71.

Parente M, Natal Jorge R, Mascarenhas T, Fernandes A, Martins J. 2009. The influence of the material properties on the biomechanical behavior of the pelvic floor muscles during vaginal delivery. J Biomech. 42:1301–1306.

Parente MPL, Jorge RMN, Mascarenhas T, Fernandes AA, Martins JAC. 2009. The influence of an occipito-posterior malposition on the biomechanical behavior of the pelvic floor. Eur J Obstet Gynecol Reproductive Biol. 144:S166–S169.

Patel PD, Amrute KV, Badlani GH. 2007. Pelvic organ prolapse and stress urinary incontinence: a review of etiological factors. Indian J Urol. 23:135–141.

Peng Q, Jones R, Shishido K, Constantinou CE. 2007. Ultrasound evaluation of dynamic responses of female pelvic floor muscles. Ultrasound Med Biol. 33:342–352.

Powell MJD. 1977. Restart procedures for the conjugate gradient method. Math Program. 12:241–254.

Rahn DD, Ruff MD, Brown SA, Tibbals HF, Word RA. 2008. Biomechanical properties of the vaginal wall: effect of pregnancy, elastic fiber deficiency, and pelvic organ prolapse. Am J Obstet Gynecol. 198:590.e1–590.e6.

Raizada V, Mittal RK. 2008. Pelvic floor anatomy and applied physiology. Gastroenterol Clin North Am. 37:493–509.

Rechberger T, Postawski K, Jakowicki JA, Gunja-Smith Z, Woessner JFJ. 1998. Role of fascial collagen in stress urinary incontinence. Am J Obstet Gynecol. 179:1511–1514.

Rivaux G, Rubod C, De det B, Brieu M, Gabriel B, Cosson M. 2013. Comparative analysis of pelvic ligaments: a biomechanics study. International urogynecology journal. 24:135–139.

Rubod C, Brieu M, Cosson M, Rivaux G, Clay JC, De Landsheere L, Gabriel B. 2012. Biomechanical properties of human pelvic organs. Urology. 79:968.e17–968.e22.

Schwertner-Tiepelmann N, Thakar R, Sultan AH, Tunn R. 2012. Obstetric levator ani muscle injuries: current status. Ultrasound Obstet Gynecol. 39:372–383.

Siegel S, Noblett K, Mangel J, Griebling T, Sutherland SE, Bird ET. 2015. Results of a prospective, randomized, multicenter study evaluating sacral neuromodulation with InterStim therapy compared to standard medical therapy at 6-months in subjects with mild symptoms of overactive bladder. Neurourol Urodynamics. 34:224–230.

Silva M, Brandao S, Parente M, Mascarenhas T, Natal Jorge R.. 2016. Establishing the biomechanical properties of the pelvic soft tissues through an inverse finite element analysis using magnetic resonance imaging. Proc Inst Mech Eng, Part H: J Eng Med. 230:298–309.

Thyer I, Shek C, Dietz HP. 2008. New imaging method for assessing pelvic floor biomechanics. Ultrasound Obstet gynecol: The Official J Int Soc Ultrasound Obstet Gynecol. 31:201–205.

Tinelli A, Malvasi A, Rahimi S, Negro R, Vergara D, Martignago R, Pellegrino M, Cavallotti C. 2010. Age-related pelvic floor modifications and prolapse risk factors in postmenopausal women. Menopause. 17:204–212.

Tumbarello JA, Hsu Y, Lewicky-Gaupp C, Rohrer S, DeLancey JOL. 2010. Do repetitive Valsalva maneuvers change maximum prolapse on dynamic MRI? Int Urogynecol J Pelvic Floor Dysfunction. 21:1247–1251.

Tunn R, Paris S, Fischer W, Hamm B, Kuchinke J. 1998. Static magnetic resonance imaging of the pelvic floor muscle morphology in women with stress urinary incontinence and pelvic prolapse. Neurourol Urodynamics. 17:579–589.

Yang J, Yang S, Yang S, Yang E, Huang W. 2009. Reliability of real-time ultrasound to detect pelvic floor muscle contraction in urinary incontinent women. J Urol. 182: 2392–2396.

Yip C, Kwok E, Sassani F, Jackson R, Cundiff G. 2014. A biomechanical model to assess the contribution of pelvic musculature weakness to the development of stress urinary incontinence. Comput Methods Biomech Biomed Eng. 17:163–176.